

Supporting information for:

**Two-photon Fluorescent Polysiloxane-Based Films with Thermal Responsive Self
Switch Property Achieved by Unique Reversible Spirocyclization Mechanism**

By Yujing Zuo, Tingxin Yang, Yu Zhang, Zhiming Gou, Minggang Tian,

Xiuqi Kong, and Weiying Lin*

[*] Prof. W. Lin, Corresponding Author

Institute of Fluorescent Probes for Biological Imaging, School of Materials Science
and Engineering, School of Chemistry and Chemical Engineering, University of Jinan
Shandong 250022, P.R. China

E-mail: weiylinglin2013@163.com

Dr. Y. Zuo, T. Yang, Y. Zhang, Dr. Z. Gou, Dr. M. Tian, Dr. X. Kong

Institute of Fluorescent Probes for Biological Imaging, School of Materials Science
and Engineering, School of Chemistry and Chemical Engineering, University of Jinan
Shandong 250022, P.R. China

Experimental

1. Materials

Polydimethylsiloxane (PDMS), and 1,3-Bis(3-aminopropyl)-tetramethyldisiloxane (MM^{NH_2}) were obtained as a commercial product and used directly. Rhodamine-B (98 %), Bisphenol A (98 %), and paraformaldehyde (96 %) were purchased from Energy Chemical Co., Ltd. and used as received. Ethanol, toluene, and dichloromethane were purchased from Tianjin Fuyu Chemical Co., Ltd. and distilled over sodium before use.

2. Characterization and measurements

Proton nuclear magnetic resonance (^1H NMR) spectra were recorded on a Bruker AVANCE 400 spectrometer using CDCl_3 as the solvent and without tetramethylsilane as an interior label. Fourier transform infrared spectra (FT-IR) were recorded on a Bruker TENSOR27 infrared spectrophotometer using the KBr pellet technique within the 4000 cm^{-1} to 400 cm^{-1} region. The contact angle was detected using a Data physics OCA-20 contact angle analyzer with distilled water as the test liquid. Scanning electronic microscopy (SEM) images were obtained using Hitachi S-4800 (7 kV). The samples were cut and coated with a thin layer of gold before the investigation. The luminescence (excitation and emission) spectra of the samples were determined with a Hitachi F-4500 fluorescence spectrophotometer using a monochromated Xe lamp as an excitation source. The excitation and emission slits measured 10 nm and 5 nm, respectively. The fluorescence imaging of cells was performed using a Nikon A1MP confocal microscope. *In situ* monitoring of the

temperature of CPU was performed on a commercial PC (Lenovo). The toxicity of **Dns-non** towards living HeLa cells was performed by the standard MTT assays.

3. Synthesis of **P1** by Mannich poly-condensation

In a 250 mL round bottomed flask, paraformaldehyde (20.0 mmol, 0.60 g), bisphenol A (**BPA**) (5.2 mmol, 1.20 g), and 1,3-Bis(3-aminopropyl)-tetramethyldisiloxane (**MM^{NH}₂**) (5.0 mmol, 1.24 g) were dissolved in a mixture of 100 ml toluene and 25 ml ethanol. The reaction mixture was heating to 110 °C and refluxed for 24 h. The solvent was evaporated under vacuum. Finally, the product was obtained as a light yellow film located in the bottom of the flask and named as **P1**.

Yield: 95 %. ¹H NMR (400 MHz, CDCl₃,ppm): δ=0.06–0.17 (m, Si-CH₃), 0.41-0.58 (m, Si-CH₂-), 1.53-1.70 (m, C-CH₃), 2.31-2.40 (m, Si-CH₂CH₂-), 2.68-2.82 (m, Si-CH₂CH₂CH₂-), 3.85-3.96 (m, N-CH₂-CH), 4.84-4.94, (m, N-CH₂-O), 6.52-7.32, (m, H proton in the benzene ring). ¹³C NMR(100 MHz, CDCl₃,ppm): δ= 0.17 (Si-CH₃), 16.3 (Si-CH₂-), 41.8 (C-CH₃), 22.4 (Si-CH₂CH₂-), 32.1 (Si-CH₂CH₂CH₂-), 50.9, (C-CH₃) 55.3, (N-CH₂-O), 82.9 (N-CH₂-CH),116-130, (C proton in the benzene ring). ²⁹Si NMR(100 MHz, CDCl₃, ppm): δ= 8.45.

P0 and **P2** were synthesized according to the synthesis procedure of **P1**. The difference is the consumption of **MM^{NH}₂**. For P0 is 1.48 g, while for P2 is 1.03 g. The NMR data of **P0** and **P2** were similar to that of P1. The GPC data were tested and listed in **Table 1**.

4. Film preparation (**Cns-non** and **Dns-non**)

A series of films were prepared by “casting” method. Each film was named as **Cns-non** and **Dns-non**. Taking **D1-non** as an example, 0.001 g rhodamine-B-methanol solution (10 ml) was added into 2.00 g **P1** dissolved in 10 ml toluene. The major of solvents were evaporated off under vacuum meanwhile the resulting mixed solution can keep flowing. Then the mixture was poured into a teflon mold and the rest solvent was evaporated off at room temperature. After 48 h, red film was obtained. Finally, the red film was put into an oven at 120 °C for 20 min, **D1-non** was obtained. **D0-non** was prepared by the similar procedure as that of **D1-non** using P0 as the film basement. While **D2-non** used **P2** as the film basement. **Cns-non** were also prepared by similar procedure as **Dns-non** using “casting” method without the consumption of rhodamine-B.

5. Measurement of swelling ratio and gel fraction

According to the classical method, the swelling ratio and the gel fraction of the samples (**Cns-non** and **Dns-non**) were tested by soaking them (W_1) in toluene for 48 h at room temperature to reach swelling equilibrium.^[1] Then, the swollen samples were removed from toluene to weigh (W_2), then the swollen networks were dried in a vacuum oven at 50 °C to a constant weight named as W_3 . Consequently, the swelling ratio and the gel fraction were determined by the following equations.

$$\text{swelling ratio} = W_2/W_1 \times 100\%$$

$$\text{gel fraction} = W_3/W_1 \times 100\%$$

where W_1 represent the original weight, W_2 is the weight after swollen, and W_3 is the dried weight after swelling of the networks, respectively.

6. Coated onto a CPU device

Coated commercial CPU (Inter ® Pentium ®) covered by post-mixed **D1-non** solution were prepared by drop casting and then cured under natural environment at room temperature for 24 h. At last, CPU was put into an oven at 50 °C for 120 min, CPU coated by **D1-non** was obtained.

7. Cell culture and imaging

HeLa cells were cultured in **D1-non** modified culture dish with DMEM medium and incubated at 37 °C in air atmosphere (5% CO₂). For fluorescence imaging, the cells were seeded into **D1-non** modified bottom dishes with appropriate density. After 24 h, the cells were dyed with 2 µM Calcein AM for 15 min. After rinsing with PBS, fluorescence images were acquired with Nikon A1R confocal microscope with 10× and 20× objective lens. [2]

8. Cytotoxicity assays.

HeLa cells were grown in the modified DMEM medium and incubated in an atmosphere of 5% CO₂ at 37 °C. Then, the cells were placed in a 96-well plate, followed by addition of increasing concentrations of **D0-non** (99% DMEM and 1% THF). The concentrations of **D0-non** were 5, 10, 25, 20 µM (n = 5). The cells were then incubated at 37 °C in an atmosphere of 5% CO₂ and 95% air at 37 °C for 24 h, followed by MTT assays. Untreated assay with DMEM (n = 5) was also conducted with the same conditions.

9. Two-photon absorption (TPA) cross sections

Two-photon absorption (TPA) cross sections were measured using the two-photon induced fluorescence method, and the cross section can be calculated by means of the followed equation:

$$\delta s = \delta r \left(\frac{\Phi_r}{\Phi_s} \right) \left(\frac{C_r}{C_s} \right) \left(\frac{n_r}{n_s} \right) \left(\frac{F_s}{F_r} \right)$$

Where s and r refer to D1-non and the reference, respectively. The terms c and n are the concentration and refractive index of the solution, respectively. F is two-photon excited fluorescence integral intensity. Φ represented the fluorescence quantum yield. r is the TPA cross-section of fluorescein in ethanol.

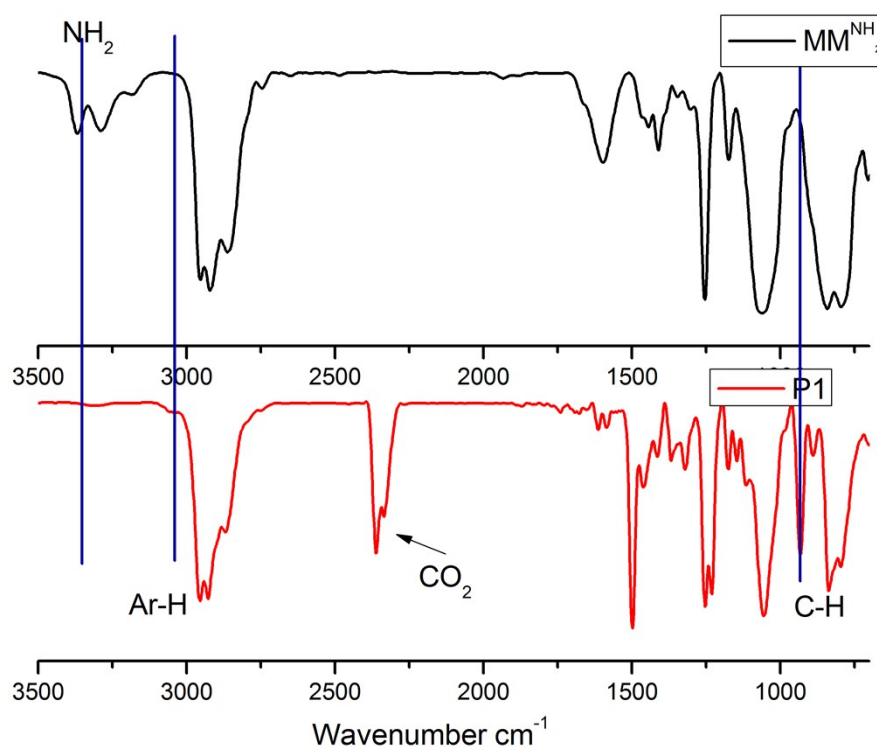


Figure S1. FT-IR spectra of MM^{NH_2} and P1 .

Note:

For Mannich condensation reaction between primary amine, formaldehyde, and phenol could develop various polybenzoxazines structures with different functionalities, we attempted to incorporate Mannich condensation reaction into polysiloxane system. As shown in **Scheme 1**, novel polysiloxane-based benzoxazine (named as **P1**) was synthesized via Mannich-condensation reaction of BPA, MM^{NH_2} and p-formaldehyde using a mixture of toluene and ethanol. The consumption of amino groups of MM^{NH_2} could be confirmed by the disappearance of N–H stretching vibrations ($3250\text{--}3400\text{ cm}^{-1}$) in **P1**, meanwhile, the and the out-of-plane bending vibrations of aromatic C-H at 960 cm^{-1} stretching vibrations of aromatic C-H ($3020\text{--}3055\text{ cm}^{-1}$) were detected in **P1**. The FT-IR spectra of **P1** and MM^{NH_2} illustrated the success formation of benzoxazine.

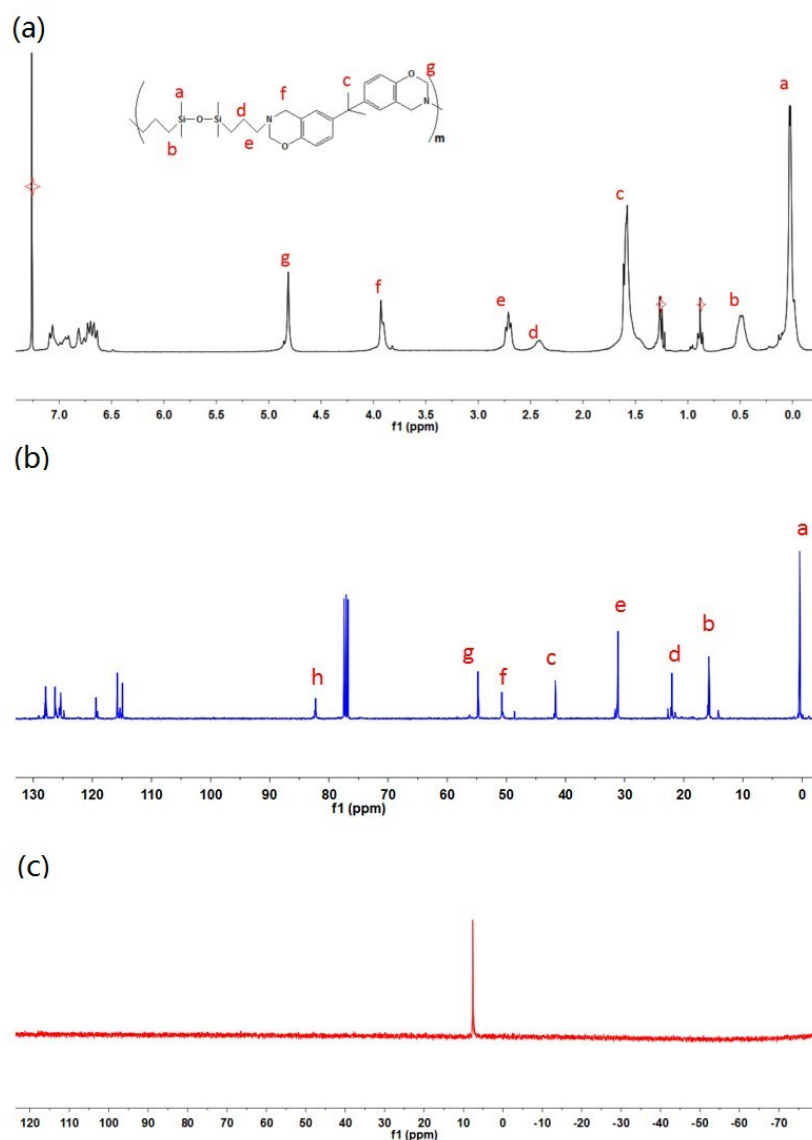


Figure S2. ^1H -NMR, ^{13}C -NMR, and ^{29}Si -NMR data of **P1**.

Note:

Figure S2(a) showed the ^1H NMR spectrum of **P1**. Typically, benzoxazine contained compounds have two single peaks with the same integration values in ^1H NMR spectra due to the proton in $-\text{CH}_2-$ groups in the benzoxazine ring. The characteristic peaks that attributed to the benzoxazine ring are founded at 3.90 and 4.90 ppm, respectively.^[3] Moreover, the ^1H NMR spectra confirm the presence of Si- CH_3 group at about 0.10 ppm, which indicated that the Si-O-Si structures were not

destroyed during the Mannich-condensation reaction. ^{13}C NMR spectra (**Figure S2(b)**) also confirmed the structures of **P1**. The characteristic carbon peaks of oxazine ring appeared at 55.3 and 82.9 ppm which are attributed to $\text{Ar-CH}_2\text{-N-}$ and $\text{-O-CH}_2\text{-N-}$, respectively. As shown in **Figure S2(c)**, the single ^{29}Si peak means the integrity of the Si-O-Si structure and the symmetry of the polymer structure of **P1**.

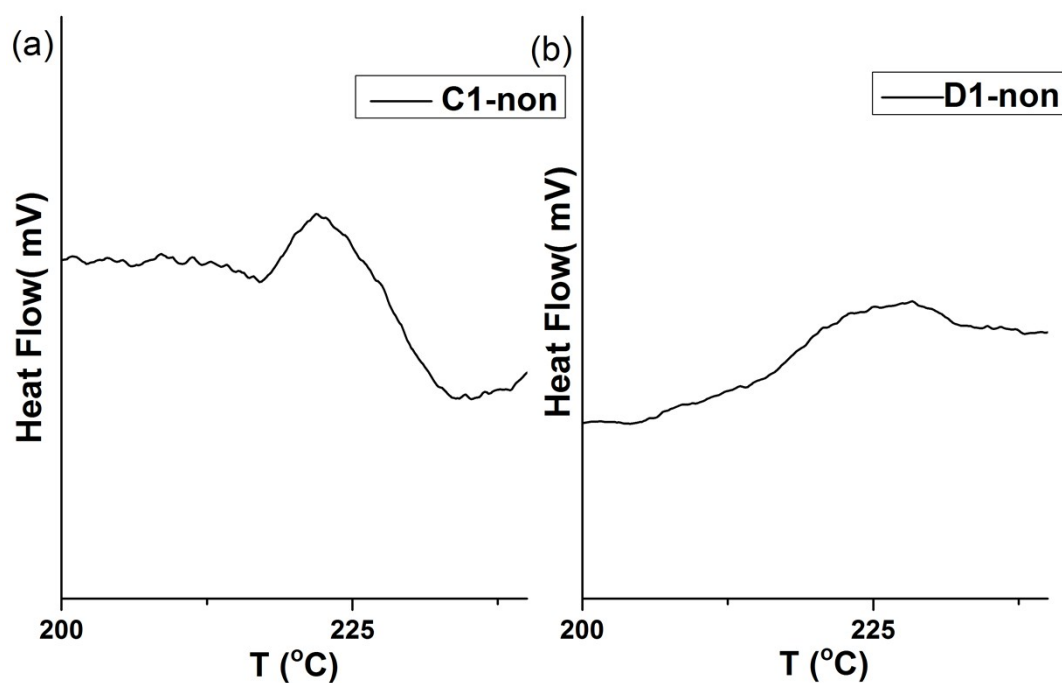


Figure S3. DSC curves of **C1-non** and **D1-non**.

Note:

It is well-known that benzoxazine group contained polymers can be cured through ring-opening polymerization with thermal treating.^[4] To investigate this process, differential scanning calorimetry (DSC) analysis was applied to monitor their thermal variation. The DSC thermograms were plotted for **D1-non** and **C1-non** were shown in **Figure S3**. As can be seen, **C1-non** exhibited an exothermic peaks at about

220 °C, which attributed to the ring-opening polymerization of benzoxazine groups. After this thermal curing step, chemical cross-linking was built. Analogously, **D1-non** also existed an exothermic peak at about 225 °C.

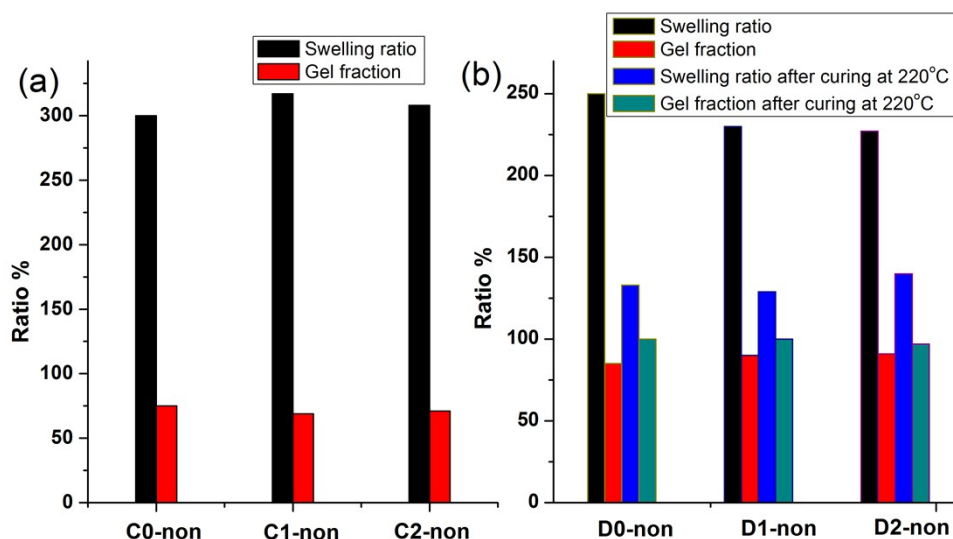


Figure S4. Swelling ratio and gel fraction of **Cns-non** (a), and **Dns-non** (b) measured in toluene.

Note:

Swelling analysis of **Cns-non** and **Dns-non**

Testing of the tensile or tear strengths of the unfilled silicones was not possible because the films obtained were hard, brittle and easy to crack during measurement. As we known, cross-linked structures are different from the linear ones for their change in solubility; thus, film **Cns-non** and **Dns-non** were put into toluene to investigate the cross-linking state. It was found that the samples only swelled but did not dissolve in toluene, which indicated physical cross-linking such as H-bonding and π - π interactions existed in these samples. In addition, the cross-linking degree of the films could be investigated by gel fraction and swelling ratio. As revealed in Figure S4(a) for the **Cns-non** system, it was found that the swelling degree and gel fraction

of **C0-non** were 300 % and 75 %, respectively. With changing the used polymer (**C1-non** and **C2-non**), the gel fractions for the cross-linked film showed subtle variation range from 69 % to 71 %. While, their swelling ratio were 300 % and 308 %. As shown in **Figure S4 (b)**, for the **Dns-non** system, it was also found that the change of polymer basement has minimal effect on the gel fraction and the swelling ratio. However, after introducing of rhodamine-B into the cross-linking films, the swelling degree decreased while the gel fraction increased, which indicated that small amount of rhodamine-B provided extra physical cross-linking sites due to its rich benzene ring structure. After a further thermal treatment at 220 °C, the swelling degree dropped markedly, along with the increasing of the gel fraction. This illustrated that the further thermal treatment bring new chemical cross-linking sites for the ring-opening of benzoxazine structure.

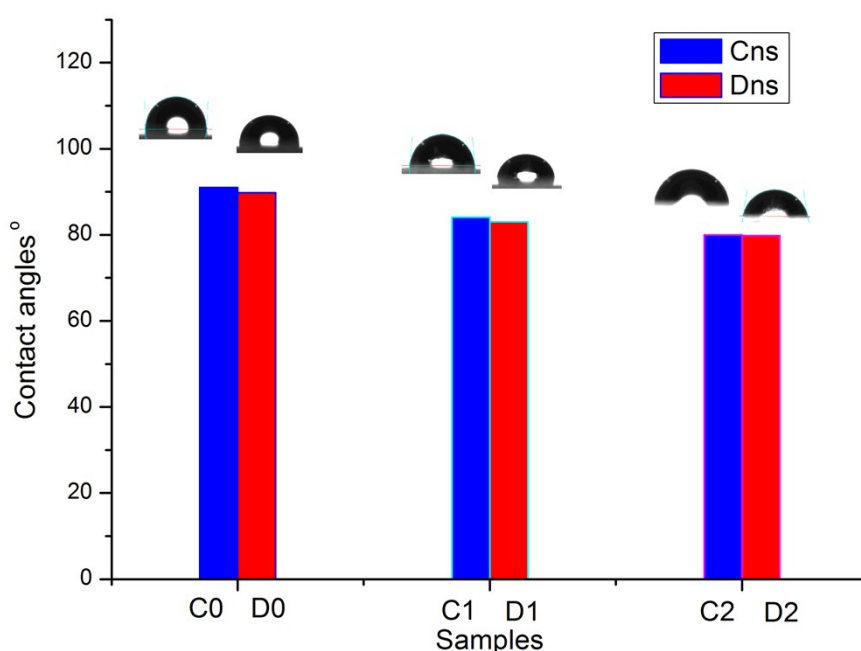


Figure S5. Contact angles of each sample (**C0-non~C2-non**, and **D0-non~D2-non**).

Note:**Contact angle measurement**

Contact angles on the surface is a very important property that is governed by both surface structure and chemical composition. Therefore, contact angle measurement was applied to investigate the surface property of the films. The contact angles were measured according to the shape of the water drop with an accuracy of 0.1° using an image analysis program. Purified water was selected as testing liquid.

Silicon-based films or elastomers are usually regarded as hydrophobic materials.^[5] However, as shown in **Figure S5**, with the introducing of benzoxazine structure, the contact angle decreased to about 80 to 100° . In addition, $-\text{NH}_2$ group also reduced the contact angles. With the increase of the consumption of MM^{NH_2} , contact angle dropped slightly. Moreover, by comparing **Cns-non** to **Dns-non**, adding a handful of rhodamine-B into the system further decreased the surface energy of the materials. In summary, the surface energy of the films could be easily tuned by merely altering the molar ratio between MM^{NH_2} and BPA.

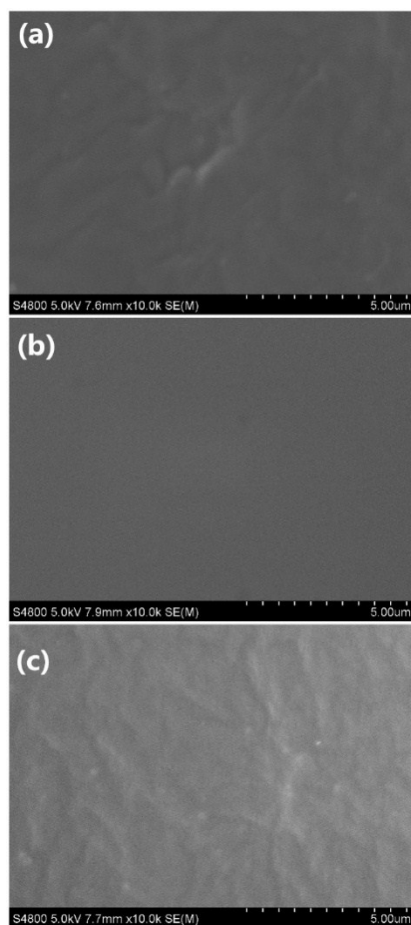


Figure S6. SEM images of **D0-non** (a), **D1-non** (b), and **D2-non** (c).

Note:

SEM (scanning electron microscope) analysis

Morphology feature is an important character of the film-like materials. The morphologies of the films were analyzed by SEM. SEM analysis results of the upper surface of **Dns-non** after heating and cooling down process are depicted in **Figure S6**. After a cycle of heating up and cooling down, a homogeneous surface was obtained. Phase separation was not observed in any of the graphs, which means that Rhodamine-B is well dispersed in the polymer matrix. The morphology of three films (**D0-non**, **D1-non**, and **D2-non**) based on different polymer did not change much. The

results indicated that casting and the followed thermal treating approach can render these materials a homogenous surface.^[6]

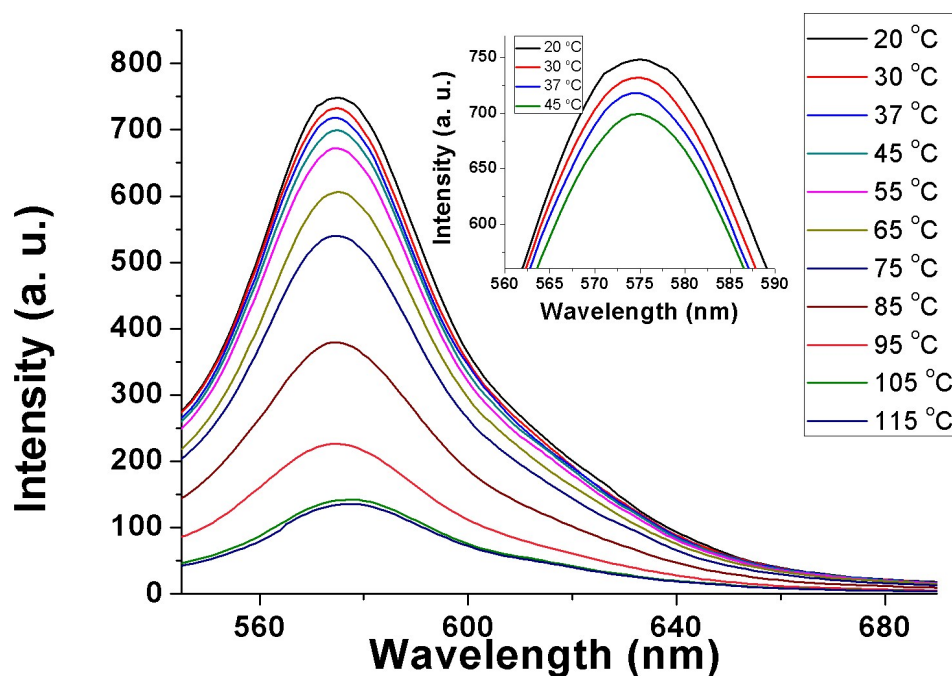
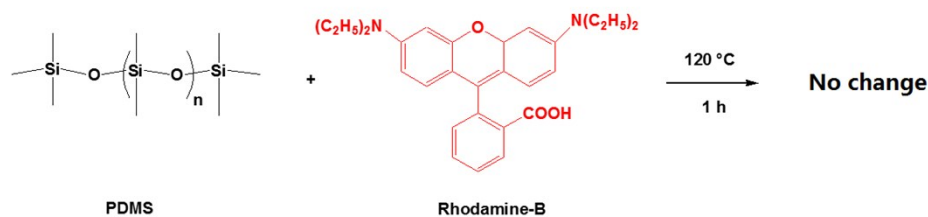


Figure S7. Fluorescence change with temperature excited at a wavelength of 520 nm for **D0-non**.

Note:

D0-non was taken as an example to study the fluorescence change with temperature. Results were illustrated in **Figure S7**. The change rate of fluorescence intensity was higher at a range of 55 °C to 105 °C. The change of the fluorescence intensity could also be detected at the temperature range at 20 °C to 45 °C, even though the change rate was not so high at higher temperature range.

(a) Control experiment:



(b) Before heating



$120\text{ }^{\circ}\text{C}$
 $\xrightarrow{1\text{ h}}$

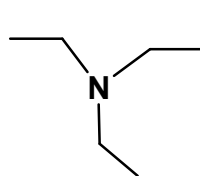
After heating



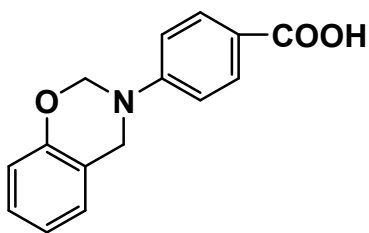
Figure S8. Illustration of control experiment between PDMS and rhodamine-B.

Note:

To exclude other factors such as the influence of Si-O-Si bond, as illustrated in **Figure S7**, a controlled experiment was established using polydimethylsiloxane (PDMS) and rhodamine-B. PDMS (2.0 g) and rhodamine-B (0.001 g) were dissolved in dichloromethane, then, dichloromethane was evaporated off at a reducing pressure. As a result, a mixture of PDMS and rhodamine-B got. The mixture was heated to 120 °C and maintained for 30 min. The result was in line with our anticipation. The luminescence of rhodamine-B did not change. The controlled experiment indicated that the fluorescence of rhodamine-B did not alter after a heating treatment and the existence of common Si-O-Si polymer chain did not affect the fluorescence of rhodamine-B.



M1



M2

Scheme S1. Illustration of model compounds **M1** and **M2**.

Note:

The mechanism of rhodamine-B transformation by tertiary amines was further proved by our own model experiment. Two kinds of tertiary amine (**M1** and **M2**) were selected to investigate the mechanism. Thereinto, **M2** was synthesized by the Mannich protocol according to the literature (*Macromolecules* 2015, **48**, 1329–1334).

Sample 1 and **Sample 2** were obtained after adding **M1** and **M2** into the rhodamine-B solution (using toluene as solvent), respectively. We wanted to inspect the effect about different tertiary amines to the fluorescence of rhodamine-B.

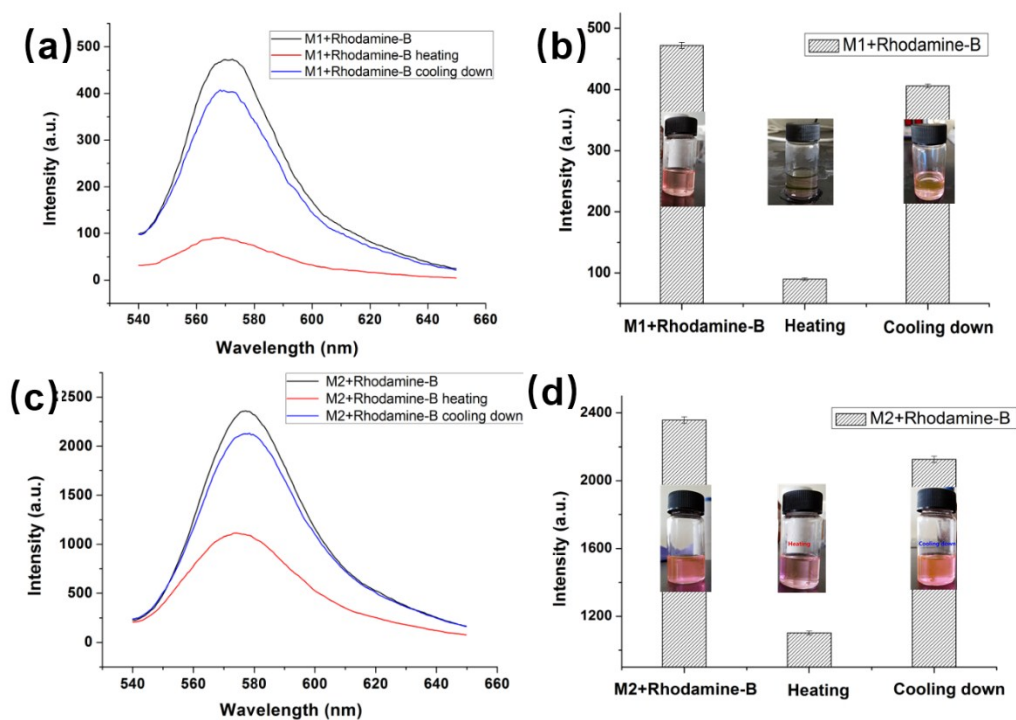


Figure S9. (a) fluorescence change of **Sample 1** after heating and cooling down process, (b) quantified fluorescence intensities for (a). The error bars represent standard deviation (\pm S.D). The inserted picture is the photograph for **Sample 1** after heating and cooling down, respectively, (c) fluorescence change of **Sample 2** after heating and cooling down process, (b) quantified fluorescence intensities for (c). The inserted picture is the photograph for **Sample 2** solution after heating and cooling down, respectively. The error bars represent standard deviation (\pm S.D).

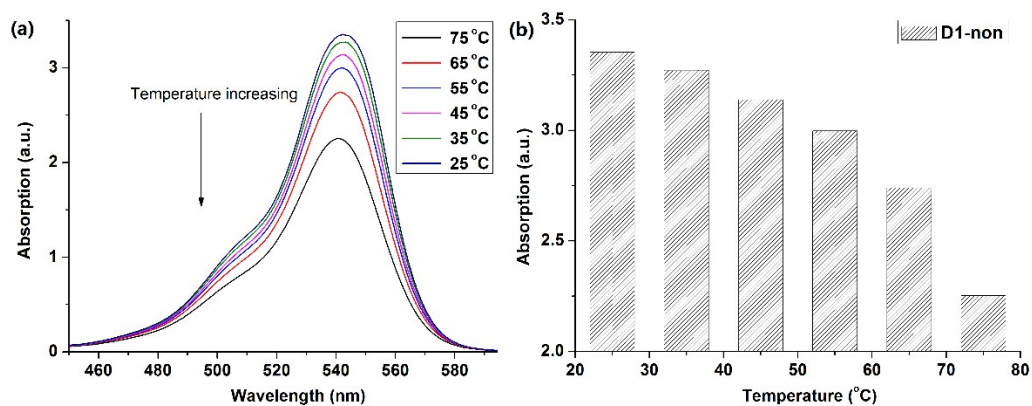


Figure S10. (a) Change of UV absorption of **D1-non** at different temperature, (b) quantified UV absorption of for (a).

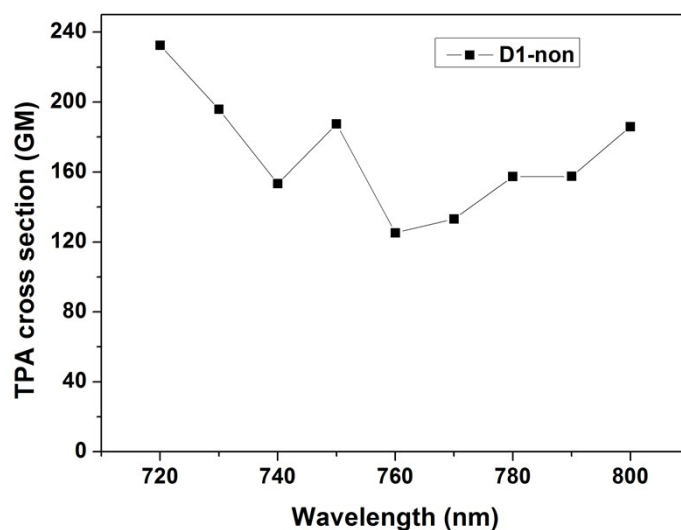


Figure S11. Two-photon cross-sections spectra for **D1-non** in ethanol. TPA cross-sections were determined using the two-photon excited fluorescence method using fluorescein as standard.

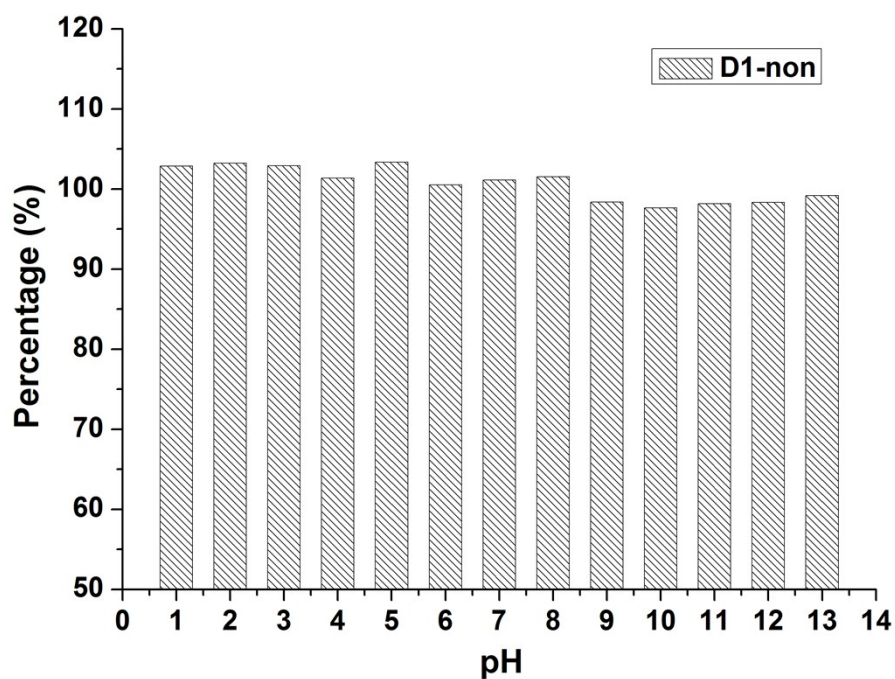


Figure S12. The plot of the normalized quantitative fluorescence intensities of **D1-non** after treated with various solutions with pH varied.

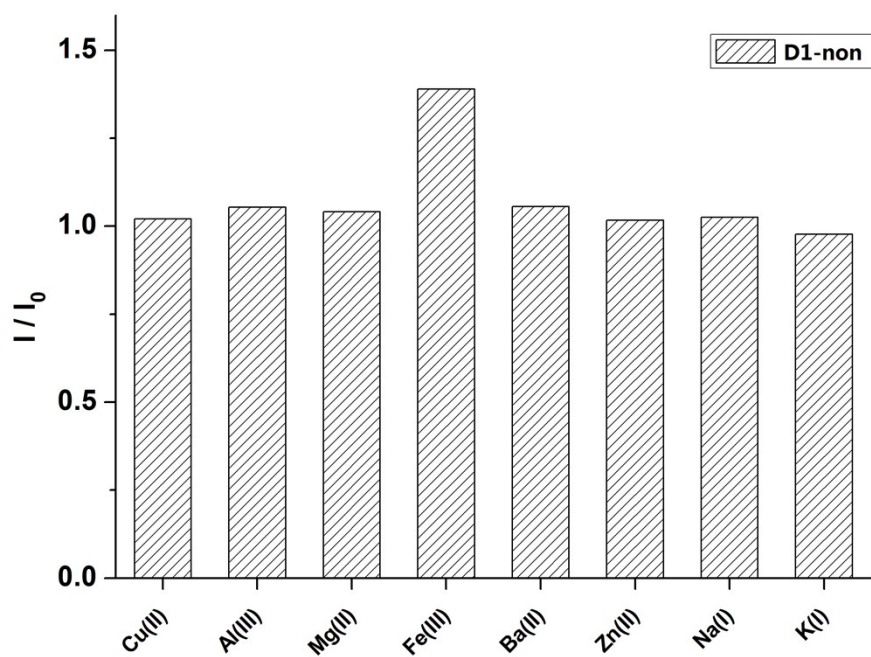


Figure S13. The plot of the normalized quantitative fluorescence intensities of **D1-non** at 580 nm after treated with various metal ions (1 mM) in water solution for 2 h. The excitation wavelength was 520 nm.

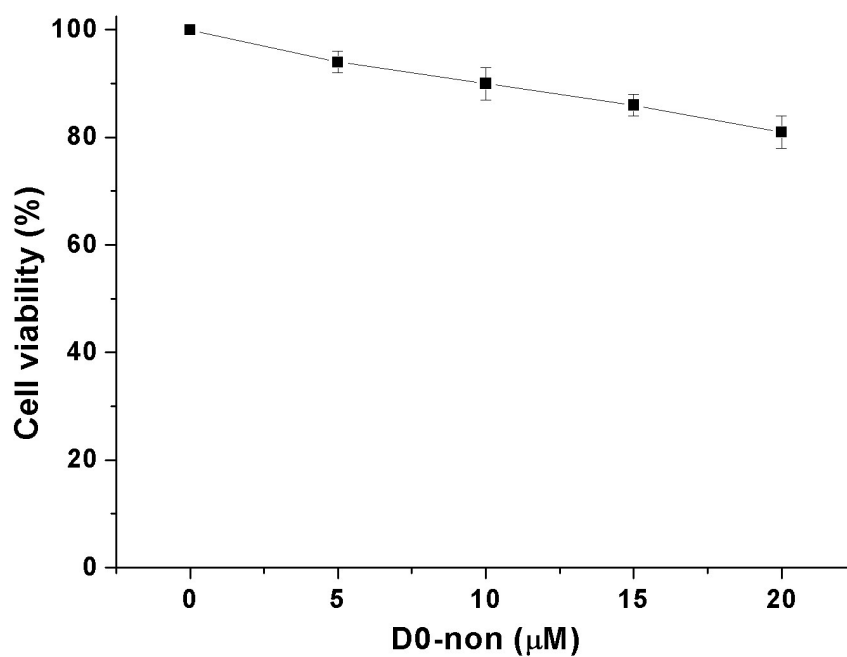


Figure S14. Cytotoxicity of **D0-non** on HeLa cells determined by MTT.

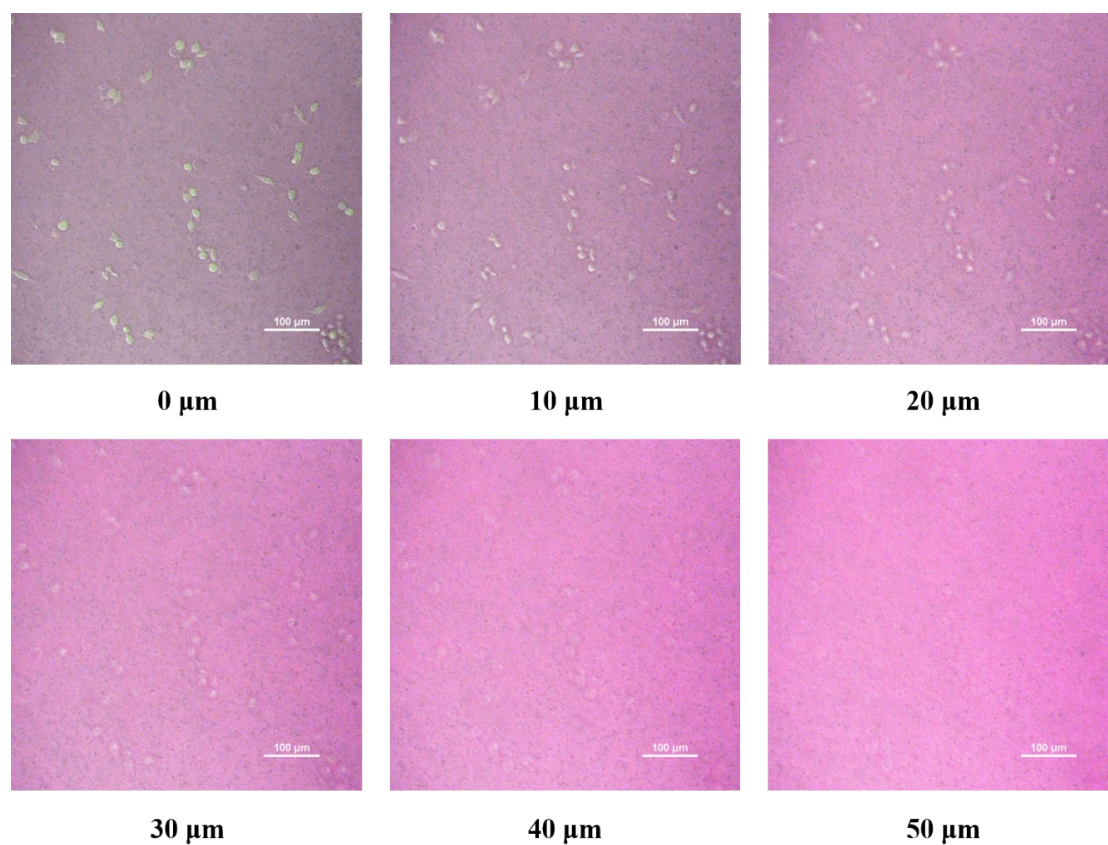


Figure S15. Fluorescence images of HeLa cells spread in **D1-non** at depths of approximately 0 to 50 μm with a magnification of 20 \times .

Table S1. GPC data on the obtained polymers

Sample name	Mn (g/mol)	Mw (g/mol)	Mz (g/mol)	PDI	Mz/Mw
P0	3100	4400	6100	1.41	1.38
P1	7700	9300	13600	1.21	1.46
P2	2800	3400	4200	1.24	1.23

References

- [1] J. Bai, H. Li, Z. Shi, M. Tian, J. Yin, *RSC Advances* **2015**, 5, 45376.
- [2] K. D. Q. Nguyen, W. V. Megone, D. Kong, J. E. Gautrot, *POLYM CHEM-UK* **2016**, 7.
- [3] A. Van, K. Chiou, H. Ishida, *Polymer* **2014**, 55, 1443.
- [4] M. Arslan, B. Kiskan, Y. Yagci, *Macromolecules* **2015**, 48, 1329; L. Dumas, L. Bonnaud, M. Olivier, M. Poorteman, P. Dubois, *European Polymer Journal* **2016**, 75, 486.
- [5] J. T. Han, D. H. Lee, C. Y. Ryu, K. Cho, *Journal of the American Chemical Society* **2004**, 126, 4796.
- [6] Y. Zuo, H. Lu, L. Xue, X. Wang, L. Wu, S. Feng, *Chemistry-A European Journal* **2014**, 20, 12924.